Gold Nanostructures from Cube-Shaped Crystalline Intermediates

Aditi Halder and N. Ravishankar*

Materials Research Centre, Indian Institute of Science, Bangalore 560 012, India

Received: November 17, 2005; In Final Form: February 3, 2006

Conventional bottom-up approaches for building nanostructures rely on the ability to synthesize nanoparticles of different shapes and sizes in a controlled manner that are then assembled to produce useful structures. Here, we present an alternate approach for producing nanostructures based on the formation of a crystalline intermediate in which the metal ion can be reduced in a controlled manner. Partial reduction of $HAuCl_4$ by a long-chain amine results in the formation of a cube-shaped crystalline intermediate in which Au is present in a +1 oxidation state. By control of the nucleation of the metal in the intermediate, a variety of nanostructures can be synthesized. Here, we present results on the formation of superlattices, hollow cubes, nanotubes, and extended hollow structures starting from the intermediate. Direct evidence for the formation of metal within the intermediate by in situ electron-beam-induced reduction in the transmission electron microscope is presented.

Introduction

Wet chemical methods are extensively used to prepare a wide variety of nanoparticles with controlled size and shape.[1−6] These nanoparticles are then used as the fundamental building blocks to create different mesoscale architectures.[7] The usefulness of nanocrystals critically depends on the ability to control their size and shape and the availability of facile routes for synthesis in large volumes. There has been a lot of interest in noble metal nanoparticles owing to their unique catalytic, optical, or bio/chemo-sensing properties.[8]

Synthesis of anisotropic nanostructures in the form of nanowires, rods, or tubes has attracted considerable attention owing to the unusual photonic and electronic properties displayed by such nanostructures.[7,9−12] Numerous recipes are available in the literature to produce structures ranging from rods,[9,13−15] nanotubes/wires,[7,10−12,16,17] cubes/polyhedra,[4,6,18,19] and hollow particles[4,20] to triangular nanoprisms.[21,22] Conventional approaches for shape control and the production of anisotropic nanostructures rely on the availability of surfactants that preferentially adsorb on specific crystallographic facets and hence modify the relative growth rates of the facets.[4,9,14,23−25] Another possibility is the formation of spatially and dimensionally constrained water pools as reverse micelles that can be used as microreactors for controlled synthesis of nanowires or rods.[13,26] Hollow nanoparticles, owing to their potential as drug carriers, have also received a lot of attention. Most methods for the formation of hollow nanoparticles rely on galvanic replacement where one noble metal is replaced by another to produce a hollow structure.[4] An alternate interesting approach is the use of the nanoscale Kirkendall effect to produce hollow structures.[20]

We provide a novel method for producing nanostructures that relies on the partial reduction of a metal salt using a weak reducing agent that leads to the formation of a cube-shaped intermediate. This intermediate, in which the metal is present in a nonzero oxidation state, serves as a crystalline nanoreactor from which the metal can be produced by reduction. Controlling the nucleation of the metal in the intermediate enables synthesis of a wide variety of nanostructures. While nucleation of the metal within the intermediate leads to the formation of "solid" nanoparticles of the order of 10−20 nm, nucleation of the metal on the surface of the intermediate enables synthesis of hollow structures. Assembly of the intermediates prior to the reduction process provides the possibility of formation of extended structures that are very difficult to obtain by other means. We have observed the formation of the cube-shaped intermediate in the case of Au, Pt, and Pd. Here, we present results for the formation of gold nanostructures starting from the intermediate.

Experimental Section

The first step involves the preparation of the crystalline intermediate. Thirty five milligrams of $HAuCl_4$ is reacted with 400 μL of oleylamine at 120 °C in the presence of 200 μL of oleic acid. The reaction is carried out in toluene medium under reflux conditions. $HAuCl_4$ is insoluble in toluene even at elevated temperatures but goes in to solution in the presence of the amine at elevated temperatures. The solution initially turns golden yellow due to the presence of Au^{3+} in solution. On continued heating, the color fades down to pale yellow to colorless implying that most of the Au is reduced to the Au^{+} state, presumably due to the formation of a Au(I)−amine complex. This intermediate is then used to prepare various nanostructures.

In a typical experiment for synthesizing superlattices of gold, 25 mL of the colorless solution (containing the intermediate) is taken in a round-bottom flask and mixed with 0.012 g of ascorbic acid followed by 50 μL of oleylamine. The mixture is heated at 65−70 °C. A gradual change in color is observed. Within 35−40 min, the whole solution turns reddish-violet indicating the formation of Au nanoparticles.

To obtain hollow nanoparticles, 50 mL of the colorless solution (containing the intermediate) is mixed with 100 μL of 1-dodecanethiol and stirred for 12 h. The resulting solution is mixed with 0.012 g of ascorbic acid and aged at room temperature. The solution separates out in to two parts after about a week. The upper, yellow-colored supernatant solution is slowly separated out and dropped on C-coated Cu grid for

* To whom correspondence may be addressed. Phone: 91-80-2293 3255. Fax: 91-80-2360 7316. E-mail: nravi@mrc.iisc.ernet.in.

10.1021/jp056648l CCC: $33.50
Published on Web 03/16/2006

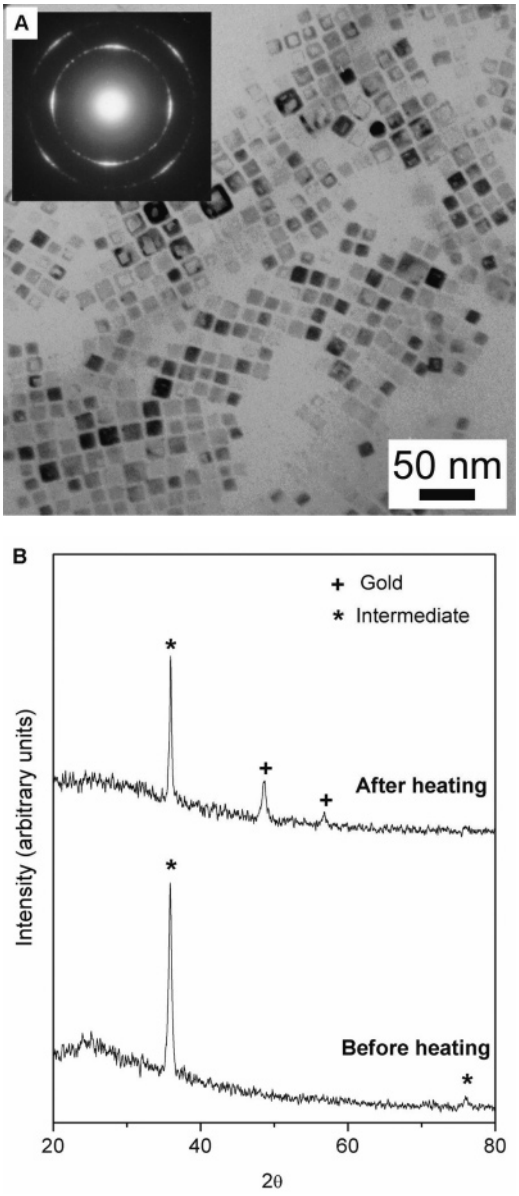

Figure 1. (A) Bright field TEM image of the cube-shaped crystalline intermediate produced on heating $HAuCl_4$ with oleic acid and oleylamine in toluene. The selected area diffraction pattern in the inset reveals the crystalline nature and the texture. The pattern can be indexed to a cubic phase with the *d* spacing of the first ring corresponding to 3.16 Å. **(**B) XRD pattern from the intermediate. Reduction of the intermediate on heating leads to the formation of fcc Au. The reduction in intensity of the diffraction peak from the intermediate is evident here.

transmission electron microscopy (TEM). This shows extended hollow structures of Au nanoparticles. In both cases, the superlattice and the extended hollow structure are the major components in the microstructure. Some amounts of spherical gold particles and unreduced intermediate cubes are also seen.

TEM analysis was carried out using a JEOL 200CX microscope operated at 160 kV.

Results and Discussion

Figure 1A is a bright field image obtained from the intermediate (colorless solution) that contains Au in the +1 state. Extended arrays of self-assembled cubes (~20−30 nm in size) are seen in all regions of this sample. The selected area diffraction (SAD) pattern in the inset reveals that the cubes are crystalline and are aligned crystallographically. The electron diffraction pattern can be indexed to a [001] zone axis from a textured cubic crystal. We have been able to successfully isolate the intermediate by dropwise addition of the solution phase to a glass plate to remove the solvent and have obtained X-ray diffraction (XRD) patterns from the same. Powder X-ray diffraction shows peaks with $1/d^2$ values in the ratio 1:2:3:4. The pattern can be indexed to a body-centered cubic (bcc) crystal structure with a lattice parameter of 4.47 Å or a simple cubic structure with a lattice parameter of 3.16 Å. From an analysis of the orientation of the faceted particle with respect to the SAD pattern, it is likely that the particles have a simple cubic structure. This is also in agreement with the *d* spacing and zone axis seen in the electron diffraction pattern. The presence of Au in the +1 state in this colorless solution has been confirmed by X-ray photoelectron spectroscopy (XPS) measurements. The formation of a Au(I)−amine complex on reducing a Au salt with an amine has been reported earlier.[27,28] However, in the above-mentioned studies, reduction was continued until the formation of Au(0) took place.

To confirm that the intermediate contains Au, we have heated to decompose the intermediate. Figure 1B is a powder XRD pattern showing the strong (110) peak of the textured cubic crystal. When the intermediate is heated, the cubes decompose to yield metallic Au as is evident from the XRD pattern in Figure 1B. There is reduction in intensity of the peak from the simple cubic phase with a concomitant increase in the intensity of the face-centered cubic (fcc) Au peaks indicating that the cubes do indeed contain Au. We have not been able to match the crystal structure of the intermediate with any known compound/complex containing gold. At this point, the chemical composition of the intermediate has not been determined. The main difficulty in determining the chemical composition of the intermediate has been to separate it out in a pure form. The presence of excess reagents or products has made this task difficult. Detailed studies are underway to obtain complete structural and spectroscopic information from the intermediate. It is interesting to note that the lattice parameter of the intermediate does not change on changing the amine to dodecylamine or octylamine. The intermediate also forms without the presence of the acid in the reaction; however the reaction is much slower indicating that the acid is essentially acting as a catalyst for the reaction. To eliminate the role of water in the reaction, we have also carried out the reaction using "dry" toluene and observed that the reaction takes place in the absence of water also.

The intermediate is stable for several days when stored at low temperatures (~10 °C) but undergoes slow decomposition/reduction on aging at room temperature to yield Au nanoparticles. The intermediate also undergoes reduction due to electron beam irradiation in the TEM. This process can be considerably hastened on increasing the electron flux by removing the condenser aperture. We have followed this reduction process in situ. Figure 2 is a sequence of images showing the conversion of the cubic intermediate to Au nanoparticles. The images were recorded at time intervals of 5 min. The condenser aperture was removed to "expose" the intermediate but was reintroduced during imaging and recording. The formation of the nanoparticles within the template is evident here. The arrows marked in Figure 2C clearly indicate the formation of gold nanoparticles. The mass thickness contrast is considerably increased on the formation of the nanoparticles (in addition to the diffraction contrast), and thus the gold nanoparticles appear much darker

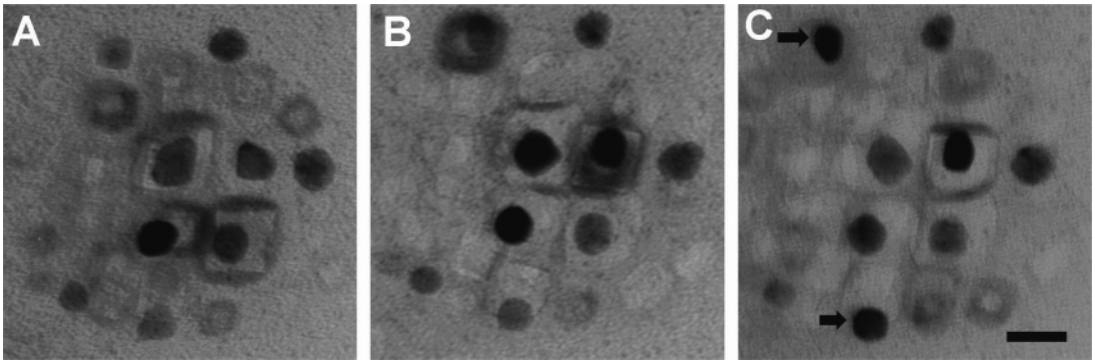

Figure 2. Sequence of in situ TEM images showing the formation of Au nanoparticles from the cube-shaped intermediate. The condenser aperture was removed to "expose" the particles and cause reduction. (A) $t = 0$ min, (B) $t = 5$ min, and (C) $t = 10$ min. The regions indicated by the arrow in (C) clearly indicate the formation of nanoparticles. Scale bar 20 nm.

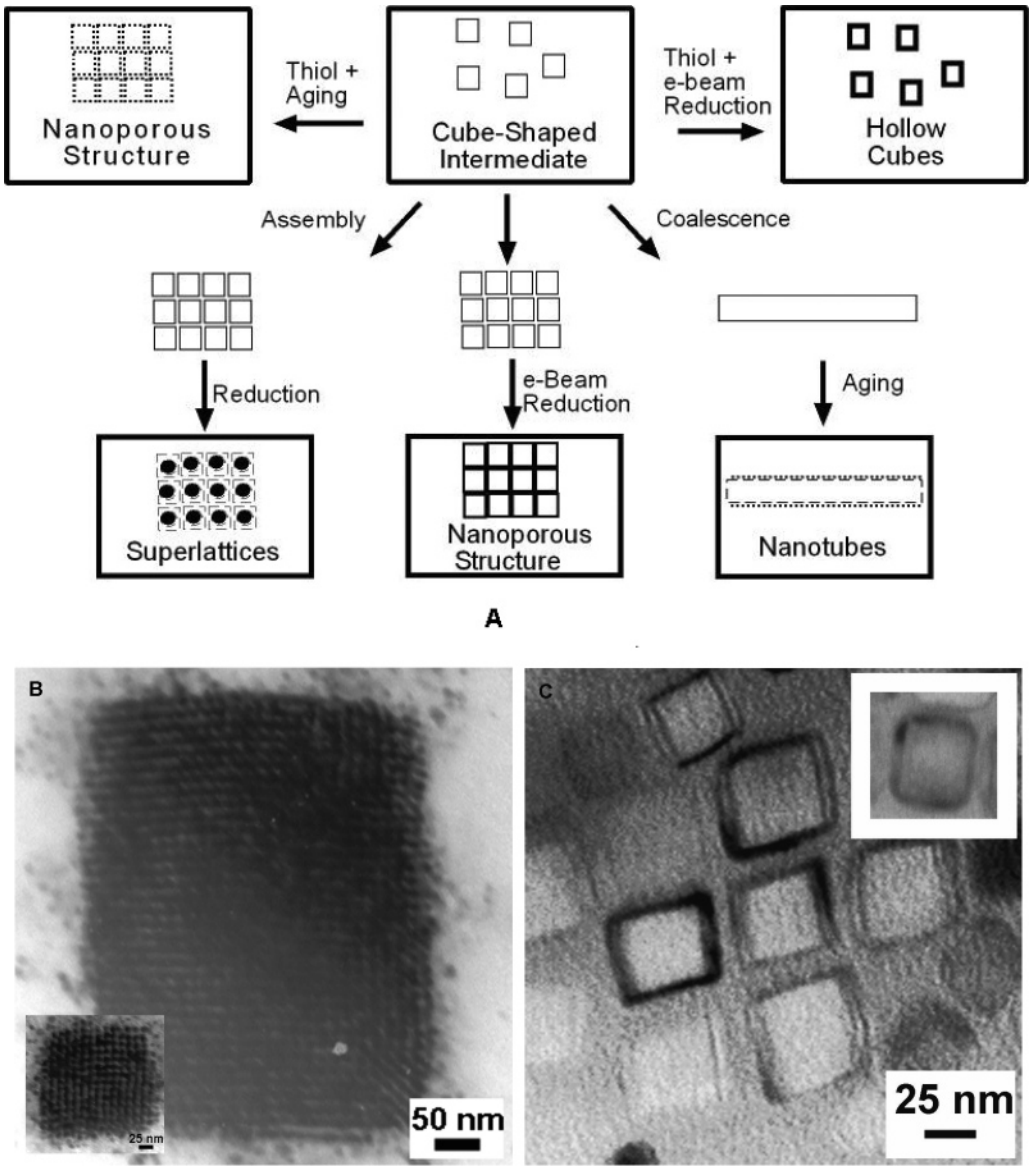

Figure 3. (A) Schematic showing the different types of nanostructures that have been obtained by controlled reduction of the cubic intermediate. (B) Large superlattices of Au are formed when the intermediate is heated slowly in the presence of a weak reducing agent (ascorbic acid). Inset shows a higher magnification image from a superlattice. (C) Hollow nanoparticles form in the presence of thiol during electron beam reduction. In this case, reduction preferentially takes place on the surface of the cubes. The cubes are slightly tilted about the vertical axis in this image. Inset shows an image from an untilted particle.

in the bright field image. The remnants of the template are also seen as an outline in the central regions of this image. As can be seen, the process is dynamic; the nanoparticles undergo subtle shape changes as is evident from the four nanoparticles in the central region of the images. There have been earlier studies of reduction of metal ions to lower oxidation states due to electron-beam irradiation in thin foils of bulk oxides.[29,30] Formation of Ag within carbon nanotubes under electron beam irradiation

has been shown earlier.[31] There has been a report on the formation of metal nanoparticles on bacterial surfaces by electron-beam-induced reduction in the TEM[32] and a more recent study on the in situ formation of gold nanoparticles in the TEM.[33]

The volume of the Au nanoparticle is considerably smaller than the original volume of the cube, and thus the particles do not inherit the cubic shape from the intermediate. Assuming that the nanoparticles are spherical, it can be estimated that the volume of the nanoparticles is less than 10% of the volume of the initial cubes. It is not clear if the reduction process is complete here.

The ability to spatially confine the metal ions into ordered domains leads to several interesting possibilities. The intermediate that serves as the template can be self-assembled in to various forms prior to the reduction process. This assembly can be controlled by changing the temperature or by adding suitable reagents that promote such an assembly. We demonstrate that a controlled reduction of the intermediate can be carried out to produce a variety of nanostructures as illustrated in the schematic (Figure 3A).

Self-assembly of the intermediate into large superlattices prior to the reduction process leads to the formation of large superlattices of Au. This process is promoted at higher temperatures (~65 °C) in the presence of a weak reducing agent such as ascorbic acid. Large cuboidal superlattices of Au of the order of several micrometers can be produced in this manner. Figure 3B illustrates one such superlattice. The second layer in the superlattice is displaced along the diagonal forming a bcc crystal. In many of the superlattices, the ordering is not perfect and there is frustration due to the presence of particles of different sizes.

The formation of superlattices with bcc structure rather than a close-packed structure can be rationalized on the basis of a process akin to crystallization of the cube-shaped intermediate in solution followed by the reduction process. We did find evidence for this in some regions where 3D superlattices of the intermediate (unreduced) were seen. Additional indirect evidence comes from the fact that the addition of a strong reducing agent such as $NaBH_4$ leads to the formation of nearly spherical Au nanoparticles with no evidence for the formation of such superlattices. The reduction by $NaBH_4$ is much faster than that by ascorbic acid, and thus there is no time for assembly of the intermediates in solution prior to the reduction process.

The Au superlattices are very similar to that of iron obtained by the reduction of $Fe[N(SiMe_3)_2]_2$.[6] However, the primary difference here is that the reduction process is not topotactic and thus the nanocrystals are randomly oriented crystallographically. This was evident from the ring pattern of Au that was seen from the thin regions of the superlattice. The superlattice could be dispersed in hexane and redeposited as monolayers on the TEM grid where it adopts the conventional hexagonal packing with nearly spherical Au nanoparticles.

Another intriguing possibility is the ability to produce hollow structures from the cube intermediate. To achieve this, we have carried out the reduction process in the presence of a thiol. Preliminary results indicate that we can indeed obtain hollow structures in the form of nanoboxes by electron-beam reduction using this approach (Figure 3C). The addition of thiol induces a striking change in the morphology of the nanoparticle obtained by electron beam reduction (compare Figure 2 with Figure 3C). This indicates that the thiol caps the intermediate cubes effectively. Nucleation of Au takes place preferentially on the surface due to the presence of the thiol owing to the strong thiol−Au interaction, and thus hollow nanoparticles are formed instead of the solid nanoparticles that form without the thiol. We believe that the presence of thiol in the medium only serves to promote nucleation of Au(0) on the surface of the intermediate. There is no chemical reaction between the thiol and the intermediate as is evident from the fact that the crystal structure of the intermediate is unchanged on adding the thiol (as evident from electron diffraction). It is to be pointed out that the hollow structure shown in Figure 3C gives a SAD pattern that corresponds to the intermediate. An estimation of the size of the Au shell that should form based on the size of the nanoparticles that formed within the intermediate (Figure 2) indicates that it should be of the order of 1 nm or less. Thus, it is clear that the reduction process is not complete here. Figure 4 illustrates another collection of particles in various stages of reduction. The particles with a thicker shell are those which are not fully reduced while those that appear bright are presumably the ones that have undergone complete reduction. It was not possible to obtain SAD information from those particles owing to their small size and extremely thin shells that are formed.

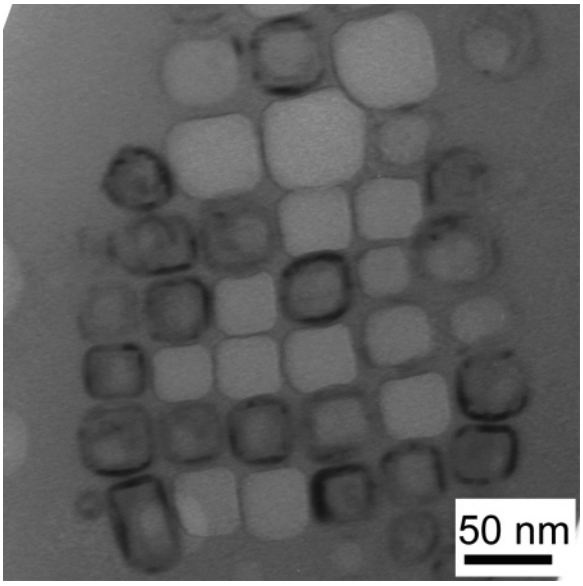

Figure 4. Bright field TEM image showing different stages of the formation of the hollow particle. The particles with a dark outline indicate partial reduction while the completely reduced particles appear bright in this image.

Nanoparticles also form on aging the solution containing the intermediate in the absence of additional reducing agent. Aging at room temperature leads to the coalescence of the cubes to produce one-dimensional (1D) structures with a square cross section. These tubes constitute about 50% of the microstructure seen in this sample. Slow reduction on aging leads to the formation of nanoparticles (1−2 nm) decorating the surface of this 1D structure to form nanotubes (Figure 5A). We believe that the process of coalescence of the intermediate is similar to that seen in the growth of Ag or CdTe wires on aging solutions containing Ag or CdTe nanoparticles, respectively.[16,17] The coalescence takes place prior to the reduction process when the Au is in the +1 oxidation state. Subsequent reduction leads to the formation of the nanotube. Addition of thiol leads to assembly of the nanocubes to form extended structures. Subsequent reduction on aging leads to preferential nucleation of Au nanoparticles on the surface of the cubes leading to extended hollow structures as seen in Figure 5B. Nanoparticles (1−2 nm) are clearly seen to decorate the cell walls. Hollow

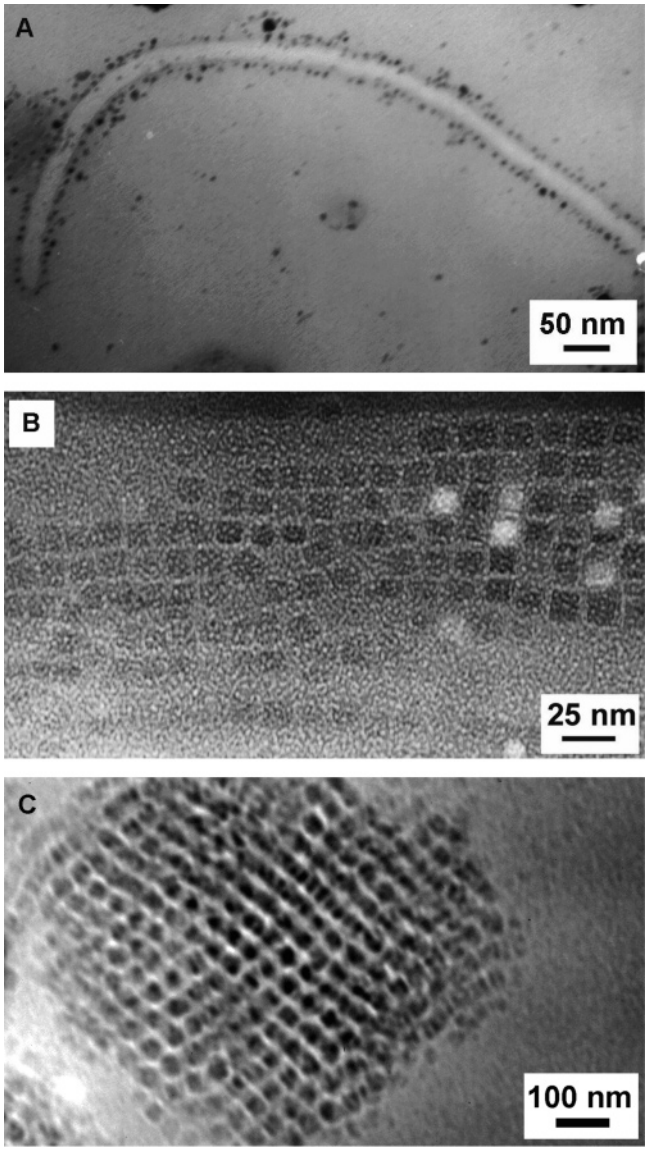

Figure 5. (A) TEM image illustrating the formation of 1D structures that are decorated by very fine (1−2 nm) nanoparticles. The tubes form due to the coalescence of the cube-shaped intermediate. Aging causes reduction to produce nanoparticles decorating the surface of the tubes. (B) Extended hollow structures (nanoporous) are produced by aging the solution in the presence of a thiol. Nanoparticles are clearly seen to decorate the cell walls of this nanoporous structure. (C) Nanoporous structure formed by electron-beam-induced reduction in the TEM. In this case, the cube-shaped intermediate assembled in the solution prior to electron beam reduction. Preferential reduction on the surface leads to the nanoporous structure seen here. The image is tilted ∼30° from the [001] orientation of the cubes. Note that (B) and (C) are bright field images. The inverted images (negative) are shown for clarity.

structures are also formed by electron beam reduction in the TEM as is shown in Figure 5C. In this case, the walls of the nanoporous structure are continuous unlike the previous case where it is decorated by nanoparticles. The ability to form meso/nanoporous metal structures as illustrated here could have possible applications in catalysis. It is interesting to note that both opal and inverse opal structures (superlattices and extended hollow structures, respectively) could be synthesized starting from the intermediate.

The procedure developed here to build nanostructures is different from conventional methods of producing and arranging nanoparticles. The discovery of a reasonably long-lived intermediate in which the metal ions are confined can be exploited in many different ways. The intermediate contains Au(I) that is spatially confined in the form of nanocubes. Nanoparticles form by the nucleation of Au(0) within this intermediate. The final nanostructure that is formed critically depends on the ability to control this nucleation process. Slow reduction using a weak reducing agent or aging at lower temperatures leads to multiple homogeneous nucleation events within the intermediate and the formation of nanoparticles of the order of 1−2 nm. The presence of thiol during reduction causes site-specific nucleation on the surface of the nanocubes leading to the formation of extended hollow structures (Figure 5B). At higher temperatures (∼65 °C), there is a pronounced tendency for assembly of the intermediate nanocubes in solution. This leads to the formation of superlattices as seen in Figure 3B. Here, we have presented only a few of the possibilities that can be realized. In principle, it should be possible to realize more complicated architectures by judiciously controlling the process parameters. Although, we have presented the formation of nanostructures in Au, we believe that this approach could be more generally applied to other systems where such intermediates can form. Preliminary results indicate that such an intermediate does form in the case of Pt and Pd also. The new approach has thrown up many new questions that are still unanswered. Work is in progress to address some of the issues.

Acknowledgment. We thank CSIR and DST, Government of India for financial support. A.H. thanks CSIR for the student fellowship (JRF). We thank Mr. Tinku Baidya and Professor M. S. Hegde, SSCU, IISc for help with XPS measurement and interpretation. We thank Professor S. Ranganathan, Professor K. Chattopadhyay, and Dr. Vijay Shenoy for critical reading of the manuscript. Valuable discussions with Mr. Bratindranath Mukherjee and Dr. Michael Rajamathi are gratefully acknowledged.

Supporting Information Available: Size distribution of cube-shaped intermediate, XRD data for the intermediate, XPS data and FTIR data, MALDI-MS, NMR, and HREM image from the intermediate. This material is available free of charge via the Internet at http://pubs.acs.org.

References and Notes

(1) Cushing, B. L.; Kolesnichenko, V. L.; O'Connor, C. J. *Chem. Rev.* **2004**, *104*, 3893.
(2) Masala, O.; Seshadri, R. *Annu. Rev. Mater. Res.* **2004**, *34*, 41.
(3) Sun, S.; Murray, C. B.; Weller, D.; Folks, L.; Moser, A. *Science* **2000**, *287*, 1989.
(4) Sun, Y.; Xia, Y. *Science* **2002**, *298*, 2176.
(5) Puntes, V. F.; Krishnan, K. M.; Alivisatos, A. P. *Science* **2001**, *291*, 2115.
(6) Dumestre, F.; Chaudret, B.; Amiens, C.; Renaud, P.; Fejes, P. *Science* **2004**, *303*, 821.
(7) Gudiksen, M. S.; Lauhon, L. J.; Wang, J.; Smith, D. C.; Lieber, C. M. *Nature* **2002**, *415*, 617.
(8) Daniel, M.-C.; Astruc, D. *Chem. Rev.* **2004**, *104*, 293.
(9) Xia, Y.; Yang, P.; Sun, Y.; Wu, Y.; Mayers, B.; Gates, B.; Yin, Y.; Kim, F.; Yan, H. *Adv. Mater.* **2003**, *15*, 353.
(10) Gundiah, G.; Rao, C. N. R.; Deepak, F. L.; Govindaraj, A. *Prog. Solid State Chem.* **2003**, *31*, 5.
(11) Rao, C. N. R.; Govindaraj, A.; Gundiah, G.; Vivekchand, S. R. C. *Chem. Eng. Sci.* **2004**, *59*, 4665.
(12) Tenne, R.; Rao, C. N. R. *Philos. Trans. R. Soc. London, Ser. A* **2004**, *362*, 2099.
(13) Murphy, C. J.; Sau, T. K.; Gole, A.; Orendorff, C. J. *MRS Bull.* **2005**, *30*, 349.
(14) Murphy, C. J.; Jana, N. R. *Adv. Mater.* **2002**, *14*, 80.
(15) Jana, N. R.; Chen, Y.; Peng, X. *Chem. Mater.* **2004**, *16*, 3931.
(16) Tang, Z.; Kotov, N. A.; Giersig, M. *Science* **2002**, *297*, 237.
(17) Korgel, B. A.; Fitzmaurice, D. *Adv. Mater.* **1998**, *10*, 661.

(18) Ahmadi, T. S.; Wang, Z. L.; Green, T. C.; Henglein, A.; El-Sayed, M. A. *Science* **1996**, *272*, 1924.
(19) Yu, D.; Yam, V. W.-W. *J. Am. Chem. Soc.* **2004**, *126*, 13200.
(20) Yin, Y.; Rioux, R. M.; Erdonmez, C. K.; Hughes, S.; Somorjai, G. A.; Alivisatos, A. P. *Science* **2004**, *304*, 711.
(21) Shankar, S. S.; Rai, A.; Ankamwar, B.; Singh, A.; Ahmad, A.; Sastry, M. *Nat. Mater.* **2004**, *3*, 482.
(22) Jin, R.; Cao, Y.; Mirkin, C. A.; Kelly, K. L.; Schatz, G. C.; Zheng, J. G. *Science* **2001**, *294*, 1901.
(23) Pileni, M.-P. *Nat. Mater.* **2003**, *2*, 145.
(24) Peng, X. *Adv. Mater.* **2003**, *15*, 459.
(25) Lee, S.-M.; Cho, S.-N.; Cheon, J. *Adv. Mater.* **2003**, *15*, 441.
(26) Lisiecki, I.; Pileni, M. P. *J. Am. Chem. Soc.* **1993**, *115*, 3887.
(27) Aslam, M.; Fu, L.; Su, M.; Vijayamohanan, K.; Dravid, V. P. *J. Mater. Chem.* **2004**, *14*, 1795.
(28) Gomez, Silvia; Philippot, Karine; Colliere, Vincent; Chaudret, Bruno; Senocq, Francois; Lecante, Pierre *Chem. Commun.* **2000**, 1945.
(29) Dahmen, U.; Kim, M. G.; Searcy, A. W. *Ultramicroscopy* **1987**, *23*, 365.
(30) Garvie, L. A. J.; Craven, A. J. *Ultramicroscopy* **1994**, *54*, 83.
(31) Ugarte, D.; Chatelain, A.; de Heer, W. A. *Science* **1996**, *274*, 1897.
(32) Mertig, M.; Wahl, R.; Lehmann, M.; Simon, P.; Pompe, W. *Eur. Phys. J. D* **2001**, *16*, 317.
(33) Kim, J.-U.; Cha, S.-H.; Shin, K.; Jho, J. Y.; Lee, J.-C. *J. Am. Chem. Soc.* **2005**, *127*, 9962.